Koopmans' condition in self-interaction-corrected density-functional theory

P. Klüpfel,[1,2,3] P. M. Dinh,[2,4] P.-G. Reinhard,[5] and E. Suraud[2,4]

[1]*Laboratoire Collisions Agrégats Réactivité (IRSAMC), CNRS, F-31062 Toulouse, France*
[2]*Laboratoire de Physique Théorique (IRSAMC), CNRS, F-31062 Toulouse, France*
[3]*Icelandic Center of Computational Science, University of Iceland, 107 Reykjavík, Iceland*
[4]*Laboratoire de Physique Théorique (IRSAMC), Université de Toulouse, UPS, F-31062 Toulouse, France*
[5]*Institut für Theoretische Physik, Universität Erlangen, D-91058 Erlangen, Germany*

We investigate from a practitioner's point of view the computation of the ionization potential (IP) within density-functional theory (DFT). DFT with (semi)local energy-density functionals is plagued by a self-interaction error which hampers the computation of the IP from the single-particle energy of the highest occupied molecular orbital (HOMO). The problem may be cured by a self-interaction correction (SIC) for which there exist various approximate treatments. We compare the performance of the SIC proposed by Perdew and Zunger with the very simple average-density SIC (ADSIC) for a large variety of atoms and molecules up to larger systems such as carbon rings and chains. Both approaches to the SIC provide a large improvement to the quality of the IP if calculated from the HOMO level. The surprising result is that the simple ADSIC performs even better than the original Perdew-Zunger SIC in the majority of the studied cases.

PACS number(s): 31.15.E−, 31.30.−i

I. INTRODUCTION

Density-functional theory (DFT) [1–3] has become a standard theoretical tool for the investigation of electronic properties in many physical and chemical systems. It provides fairly reliable results with moderate computational effort. Practical implementations of DFT employ simple and robust approximations for the exchange and correlation functional. The simplest one is the local-density approximation (LDA), which has been proven very useful in calculations of electronic structure and dynamics. Typical applications stretch from first-principles calculations of the electronic ground state and molecular geometries [4], over dynamic studies of near-equilibrium situations (e.g., optical response, direct one-photon processes), to highly nonlinear dynamical scenarios [5–7]. However, the LDA is plagued by a self-interaction error [8]: The Kohn-Sham (KS) mean field is computed from the total density which includes all occupied single-particle states, including the state on which the LDA field actually acts. The locality of the energy functional leads to a wrong asymptotic KS field. This is still a great hindrance in many applications, for instance a possibly large underestimation of the ionization potential (IP) and the absence of Rydberg or excitonic series in the static KS spectrum [9,10], the polarizability in chain molecules [11,12], or the spectral and fundamental gap in solids [13,14]. Another challenging application is the description of molecules or clusters deposited on surfaces [15,16]. In dynamic scenarios, the self-interaction error also dramatically affects ionization dynamics, especially close to thresholds, e.g., in a time-dependent DFT model of electron emission [7,17–19].

In practice, the wrong asymptotics of the KS field stems from an incomplete cancellation of the self-interaction error between the Hartree potential and the approximate exchange and correlation field. Such a spurious self-interaction is avoided by a complicated nonlocality in exact KS DFT [20–22]. For the total energy, the requirement for nonlocality can be incorporated into gradients of density leading to the generalized gradient approximation (GGA) [23–25]. This approximation indeed served to lift DFT to a quantitative level in molecular physics and chemistry problems, but is insufficient to restore proper asymptotics of the mean field.

Although there are approaches to improve the asymptotic KS potential [26] those are often too demanding for practical calculations, in particular in the time domain. The aforementioned examples show that there is still a need for robust and practical approaches to improve on the asymptotic KS potential, such as the self-interaction correction (SIC).

The original proposal for a SIC [8,27] by Perdew and Zunger (PZ) has been developed at various levels of refinement and proved to be useful over the years, in particular for structure calculations in atomic, molecular, cluster, and solid-state physics; see, e.g., [28–35]. This original PZSIC scheme, however, leads to an orbital-dependent mean field which causes several formal and technical difficulties [29,32,33,35, 36]. There are attempts to circumvent the orbital dependence by treating the SIC with optimized effective potentials [37]; for a review, see [38]. However, the resulting formalism is, again, quite involved and usually treated approximately [39]. A very robust and simple SIC is the average density SIC (ADSIC) which was proposed already very early [40], taken up in [41], and used since in many applications to cluster structure and dynamics in all regimes.

The ADSIC takes the total density divided by the electron number as a reference for the single-electron density in each state. Nonlocality is incorporated in the scheme by the global density integral providing the total particle number. However the ADSIC functional, unlike that of the PZSIC, is a functional of the total density and thus the subsequent mean field is not orbital dependent anymore. Having the correct total charge, the ADSIC provides the proper asymptotics for the mean field. It is argued that the approximation by one and the same (average) single-particle density for each state is applicable only in simple metals where all electronic states cover the same region of space, that is, in the case of a cluster, the whole cluster itself [41]. Later studies revealed that the

ADSIC is also an efficient correction scheme for nonmetallic systems with delocalized electrons, such as organic molecules [42,43].

The aim of this paper is to investigate the performance of the ADSIC in direct comparison to the PZSIC for a large variety of atoms and molecules in their ground states. The sample covers systems of different binding types, and not only metallic ones. We will compare the ADSIC with just a DFT treatment using (semi)local functionals and with the PZSIC, and also occasionally with a Hartree-Fock treatment. The comparison focuses on the proper description of the IP. We start from atoms as elementary building blocks of any molecule, proceed to a large variety of molecules from simple dimers to more complex organic structures, and finally discuss carbon rings and chains with a systematic variation of sizes. Such a strategy allows us to cover various binding types but also various geometries and even dimensionality.

II. IONIZATION POTENTIAL

A. Definitions

The key quantity of this survey is the ionization energy I, commonly called the ionization potential. The IP of an N-electron system is given by the energy difference

$$I \equiv I_\Delta = E(N-1) - E(N). \tag{1}$$

The energies $E(p)$ correspond to ground-state configurations of a p-particle system in a given external potential, typically the Coulomb potential created by the nuclear charges. Both energies, $E(N)$ as well as $E(N-1)$, are fundamental observables in ground-state DFT and so is their difference, the IP. DFT should thus allow one to calculate the IP of electronic systems. A distinction has to be made here. The definition of an IP is unique in atoms. In molecules, however, we distinguish vertical and horizontal IPs. The vertical one considers the energy difference after the removal of one electron for frozen atomic positions. This typically corresponds to photon-induced fast emission processes. The horizontal IP is built from the difference between fully relaxed molecular configurations. It accounts for the energy change on a long time scale on which all molecular relaxation processes are finalized. We will consider throughout this paper the vertical IP which accounts for fast electronic processes and which is closely related to the properties of the electronic ground state of the mother system, in particular to the highest occupied molecular orbital (HOMO).

In the exact electronic ground state, the asymptotic decrease of the ground-state density n is related to the IP by

$$n(\mathbf{r}) \overset{|\mathbf{r}| \to \infty}{\sim} \exp[-2\sqrt{2I}|\mathbf{r}|]. \tag{2}$$

In an exact KS DFT, the asymptotic decay of the total density is defined merely by the highest occupied KS orbital, i.e., the HOMO [4]. In combination with the proper asymptotic behavior of the KS potential $[v_s(\mathbf{r}) \to 0]$, the ionization energy can thus be related to the single-particle energy of the HOMO:

$$I \equiv I_\varepsilon = -\varepsilon_{\text{HOMO}}. \tag{3}$$

For an exact exchange-correlation functional, both definitions of the ionization energy, Eqs. (1) and (3), coincide, i.e., they obey $I_\Delta = -\varepsilon_{\text{HOMO}}$. The identification of the negative HOMO energy with the IP was referred to as Koopmans' theorem [44] long before the fundamental concepts were extended rigorously to the framework of DFT [45,46]. For approximate energy functionals Koopmans' condition does not necessarily hold [2] and the deviation from the ideal behavior can be used to define the non-Koopmans' (NK) energy

$$\Delta E_{\text{NK}} = I_\varepsilon - I_\Delta. \tag{4}$$

A value $\Delta E_{\text{NK}} = 0$ signals that Koopmans' theorem is fulfilled. In such a situation, the properties of the HOMO level are closely related to ionization and electron emission. We know that the LDA produces rather large violations of Koopmans' theorem and thus exhibits a sizable ΔE_{NK}. The SIC should reduce that, and the amount of reduction is one measure of the efficiency of the actual SIC scheme.

It is also interesting to compare the performance of a calculation with respect to data. Thus we consider in addition to the NK energy the bare error in the IP relative to experiments or other reference data. As we have two definitions of the IP, there are two bare errors in an approximate theory:

$$\Delta I_\varepsilon = I_\varepsilon - I_{\text{ref}}, \quad \Delta I_\Delta = I_\Delta - I_{\text{ref}}. \tag{5}$$

An experimental reference energy may be hampered by uncertainties, as ionic relaxation throughout the ionization process can lead to situations which lie between the idealized vertical IP (for very fast ionization) and the horizontal one (for very slow ionization). Here only the vertical IP in the ground-state geometry is considered. Reliable atomic coordinates for small molecules are given by the second-order Møller-Plesset (MP2) optimized structures as provided in the Gaussian 2 (G2) data set [47]. G2 theoretical and experimental energies may differ by several tens to hundreds of meV [48]. This error can be considered negligible on the scale of the expected errors, stemming from the approximate nature of the used exchange-correlation functionals and the use of pseudopotentials [49]. Experimental data for vertical IPs therefore appear as a safe choice of reference [50].

In contrast to the errors in the IP (5), the NK energy does not require any reference data that may be hampered by experimental uncertainties. It therefore provides a rather rigorous criterion for the quality of energy-functional approximations.

B. Impact of a proper description of the IP

The two definitions (1) and (3) for the IP are equally justified in an exact calculation. However, for (semi)local functionals (as in the LDA and GGA), it is usually found that only the energy difference (1) can be used to extract a good estimate for the IP. The estimate (3) from the single-particle spectrum requires the proper $1/r$ asymptotics of the exchange-correlation potential (for neutral systems). This is not provided in calculations based on typical semilocal functionals.

While energy differences often allow reliable estimates already with semilocal functionals, they require two calculations, which is more involved than a straightforward extraction from the HOMO level. This alone would not be *a priori* a major hindrance. But there are many situations where the extraction
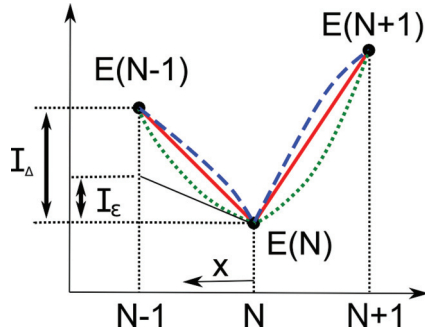
FIG. 1. (Color online) Illustration of the ground-state energy E as a function of fractional occupation number ν. The IP from the HOMO level, I_ε, corresponds to the left-handed derivative (slope = thin black line) of the energy at $\nu = N$. The IP from energy differences, I_Δ, is associated with the exactly linear behavior (red, heavy solid line). The LDA result provides a smooth curve (green, dotted line). The Hartree-Fock result (blue, dashed line) also has a discontinuous derivative at $\nu = N$ as the exact trend, but tends to overestimate the kink.

via energy difference is not an option: In periodic calculations (e.g., on surfaces), a rigorous calculation of the IP (called the work function in this case) from an energy difference is hard to achieve because one cannot easily model a single excess charge in a periodic setup. The same situation applies for calculation of band gaps in solids. In dynamical situations, as described by time-dependent DFT, an accurate modeling of the ionization process requires an accurate static single-particle spectrum. As the propagation of the single-particle states is driven by the time-dependent KS Hamiltonian, the energy difference between its spectrum and a proper position of the IP is more important than the total energy. Ionization properties are also mostly defined by the HOMO level, which thus has to be correctly described.

A way to illustrate the self-interaction error is to consider the energy $E(\nu)$ as a function of a fractional particle number ν. Note that, while fractional electrons of course do not exist, a fractional particle number can be interpreted as the average over an ensemble of systems with integer occupation numbers. In time-dependent DFT, it rather refers to a level depletion corresponding to scattering into continuum states (which are not localized within the simulation volume). The ionization process proceeds as $\nu = N \longrightarrow N-1$. An exact functional produces a linear behavior [20], as

$$E(\nu) = (1-x)E(N) + xE(N-1), \ \ x = N - \nu \in [0,1].$$
(6)

A similar linear behavior is also observed for ionization from an anion to the neutral system ($N + 1 \longrightarrow N$). This exact $E(\nu)$ is shown as the (red) solid line in Fig. 1.

The remarkable feature is a discontinuous derivative, that is, a kink, at $\nu = N$. Semilocal functionals deal with smooth functions (no kinks, no discontinuities) and produce smooth trends as shown in the (green) dotted line. The definition (3) of the IP through the HOMO energy coincides with the slope of the total energy for fractional particle numbers at $\nu \nearrow N$:

$$I_\varepsilon = - \left. \frac{dE}{d\nu} \right|_{\nu \nearrow N}$$
(7)

as indicated in the figure. The linear trend of the exact energy naturally guarantees $I_\varepsilon = I_\Delta$, while the convex curve from the LDA necessarily implies $I_\varepsilon < I_\Delta$.

The (blue) dashed line in Fig. 1 finally shows results from exact exchange in the Hartree-Fock (HF) method. A full HF calculation is free from self-interaction error. Thus it qualitatively yields the correct result, namely, the kink at $\nu = N$. However, it differs from the linear trend in between integer particle numbers. This leads to an overestimation of the IP from the HOMO, $I_\varepsilon > I_\Delta$. We will address this question in the last example of carbon chains; see Sec. IV E.

III. VARIOUS SCHEMES FOR AN SIC

As the SIC is rather an *ad hoc* measure to cure the self-interaction problem, various recipes and approximations are used, depending on the field of application. In this section, we briefly summarize the PZSIC and ADSIC which we will use later on in an extensive comparison of results.

A. Perdew-Zunger SIC

As already mentioned in the Introduction, a very popular approach to the definition of a one-particle self-interaction error and a corresponding correction was presented by Perdew and Zunger [8]. The self-interaction error is given by accumulating the contributions from the individual orbital densities $n_i(\mathbf{r}) = |\varphi_i(\mathbf{r})|^2$ for a set of single-particle states $\varphi^N = (\varphi_1, \ldots, \varphi_N)$. It reads

$$E_{\mathrm{SI}}[\varphi^N] = \sum_{i=1}^{N} (E_{\mathrm{H}}[n_i] + E_{\mathrm{xc}}[n_i]),$$
(8a)

where E_{H} is the Coulomb Hartree energy and E_{xc} is the density functional for exchange and correlations. Note that this is not a functional of density alone. In fact, $E_{\mathrm{SI}}[\varphi^N]$ depends on the details of the orbitals. The PZSIC is defined by subtracting the self-interaction error from the original functional, i.e.,

$$E_{\mathrm{PZSIC}}[\varphi^N] = E_{\mathrm{H}}[n] + E_{\mathrm{xc}}[n] - E_{\mathrm{SI}}[\varphi^N],$$
(8b)

where $n = \sum_{i=1}^{N} n_i$ is the total electronic density.

The mean-field equations are derived in a straightforward manner by variation of the SIC energy E_{PZSIC} with respect to the occupied single-particle orbitals φ_i. It turns out that the mean-field Hamiltonian depends explicitly on the particular single-particle state on which it acts. This emerges because the PZSIC energy functional is not invariant under unitary transformations among the occupied states. There are several ways to deal with such a state-dependent Hamiltonian [28–31]. A particularly efficient way is to use two different sets of single-particle states which are connected by a unitary transformation among occupied states. That is actually the solution scheme which we are using; for details, see [51]. In this approach, the HOMO level is defined as usual, in the basis set which diagonalizes the Hamiltonian matrix.

B. Average density SIC

The average density SIC starts from the SIC energy (8b) and simplifies it by assuming that indistinguishable electrons are represented by equal single-particle densities. In such an

extreme simplification, one expresses them as the one-particle fraction of the total spin density $n_i(\mathbf{r}) = n_{\sigma_i}(\mathbf{r})/N_{\sigma_i}$, where σ_i is the spin of state i and N_{σ_i} is the number of particles with spin σ_i. In such a scheme, the standard PZSIC functional is represented by the ADSIC functional:

$$E_{\mathrm{ADSIC}}[n_\uparrow, n_\downarrow] = E_{\mathrm{H}}[n] + E_{\mathrm{xc}}[n]$$
$$- \sum_{\sigma \in \{\uparrow, \downarrow\}} N_\sigma \left(E_{\mathrm{H}}[n_\sigma] + E_{\mathrm{xc}}[n_\sigma] \right), \quad (9)$$

where $n = n_\uparrow + n_\downarrow$. This is a spin-density functional and can be treated in the same manner as any LDA or GGA scheme. This makes it extremely simple and efficient to use in atomic and molecular systems. However, the ADSIC functional contains a cumbersome nonlocality as it explicitly depends on the particle number $N_\sigma = \int d^3\mathbf{r}\, n_\sigma(\mathbf{r})$. This inhibits its application in periodic systems, where N_σ is infinite.

IV. RESULTS

A. Numerical scheme and pseudopotentials

We performed symmetry-unrestricted calculations using a representation of the single-particle wave functions on a Cartesian coordinate-space grid with a spacing of 0.2 Å. We accounted for spin polarization whenever necessary, but ignored noncollinear spin configurations. Densities and fields were represented on a refined grid of 0.1 Å to account for the higher Fourier components in products of single-particle states. The core electrons are handled within the frozen-core approximation by a real-space implementation of the projector augmented wave (PAW) method [52] using a development version of GPAW [53]. The projectors and partial waves of the PAW method are taken as provided within the GPAW repositories for bare LDA exchange and correlation, i.e., without accounting for a SIC. During the energy optimization, we apply a strict preconditioned gradient scheme, i.e., we do not mix occupied with unoccupied states by explicit diagonalization of the Hamiltonian in the iterated subspace. Using this procedure, we do not have to decide which orbitals to occupy, based on symmetry considerations in the case of small HOMO-LUMO (lowest unoccupied molecular orbital) gaps and systems with partially filled angular momentum shells. For the evaluation of I_ε, we used the HOMO (no matter which spin it has) and compared to the spin configuration of the cation that arises from fully removing an electron from the corresponding spin channel in I_Δ. On the LDA level, this procedure was in agreement with explicit optimization of the magnetic moment of the cation state (determined by explicitly trying different spin configurations). Hence, the problem of an unknown strength of the effective Kohn-Sham magnetic field in open-shell systems is avoided, as discussed in [54].

This corresponds to using pseudopotentials developed for LDA applications in the context of the PZSIC or ADSIC without readjustment of the pseudopotential parameters. This minor inconsistency is acceptable in various applications of the SIC [32,55,56]. Here such an improvement is avoided in favor of using a unique set of pseudopotentials for all energy functionals.
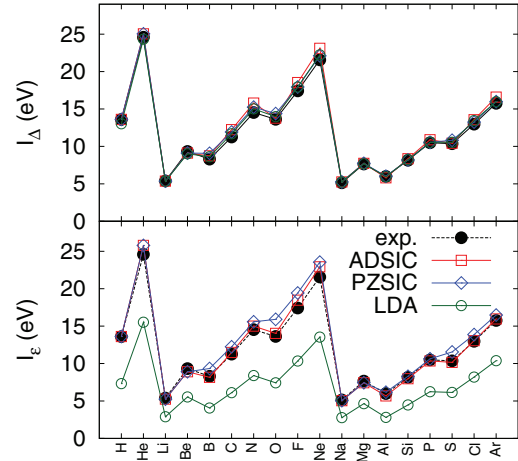

FIG. 2. (Color online) Ionization potentials I_Δ from Eq. (1) and I_ε from Eq. (3) for neutral atoms from hydrogen to argon and different approaches to the self-interaction correction: Average density SIC (squares), Perdew-Zunger SIC (diamonds), and the uncorrected local-density approximation (open circles). Experimental data are displayed as closed circles [50].

For the following survey, we show results from the LDA using the Perdew-Wang 1992 (PW92) parametrization [57]. For most of the examples below, we have also performed GGA calculations with the PW91 functional [24]. Even though the GGA slightly improves the overall quality of the IP, in particular if calculated from energy differences, with very few exceptions, the effect of the gradient dependence is less than 0.5 eV. Thus it neither affects the overall magnitude of errors or changes the general trends that are discussed in the following sections. We therefore focus on the LDA part in this survey.

B. Atoms

The first step is to investigate the performance of both SIC approaches for atoms. The latter are the basic building blocks of molecules and solids. Thus they must be correctly described before we can proceed to more complex scenarios. The electronic structure of atoms incorporates single-electron states with similar shapes but different spatial extensions. Thus atoms are a critical test case for SIC which is known to strongly depend on the level of localization.

Figure 2 shows the IP as calculated for neutral atoms from hydrogen ($Z = 1$) to argon ($Z = 18$). All methods yield very similar IPs if it is evaluated as I_Δ, i.e., as the energy difference (1). The results differ more for I_ε computed from the HOMO according to Eq. (3). Here, the bare (semi)local energy functionals underestimate the ionization energy by 30%–40%. The defect is well known and can be traced back to the wrong asymptotic behavior of the exchange-correlation potential for $|\mathbf{r}| \to \infty$ [8]. Obviously, both SIC approaches cure the problem and yield excellent agreement with experimental data. The ADSIC is slightly superior in the case of open-shell atoms, while the PZSIC slightly overestimates the IP. Accounting for density gradients by using the PW91 approximation to the exchange-correlation functional [24] (not shown here) has an insignificant effect for both I_Δ and I_ε. The results do not sufficiently differ to justify a separate plot.
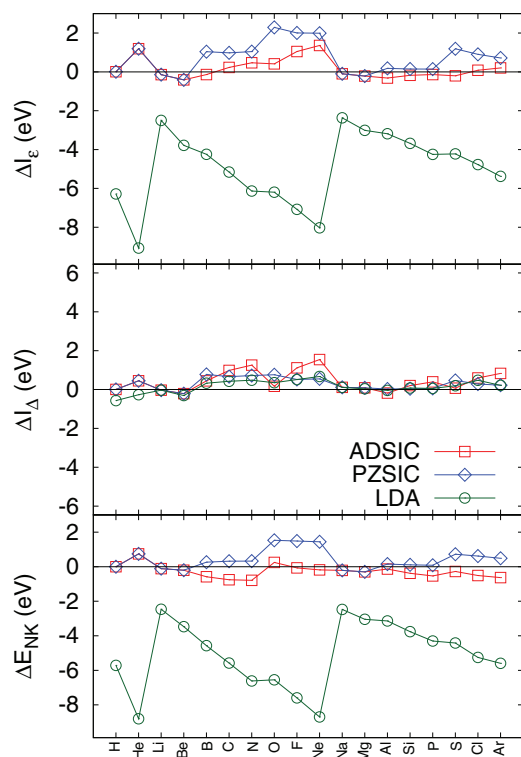
FIG. 3. (Color online) Errors in calculated IPs compared with experimental values for the series of atoms depicted in Fig. 2. Top and middle panels: errors from I_ε and I_Δ, respectively, according to Eq. (5). Bottom panel: non-Koopman's energy defined in Eq. (4).

Figure 3 shows the same data as in Fig. 2 but in terms of errors with respect to experimental data and of the NK energy. This reveals some differences between the PZSIC and ADSIC where, somewhat surprisingly, the technically much simpler ADSIC visibly yields smaller NK energies and errors ΔI_ε.

At this point, it is worth recalling that the ADSIC scheme can be derived as an approximation to the PZSIC, assuming the most delocalized representation of the single-particle densities. In the ADSIC, orbitals extend over the whole atom, in stark contrast to the localized orbitals that are commonly found in PZSIC calculations [33]. It thus appears that a significant higher level of delocalization is actually desirable, which confirms previous concerns that PZSIC orbitals are too localized.

C. Simple molecules

As a next step, we consider simple molecules, such as many dimers, and a few more complex ones. The selection has been adapted from [25]. It covers systems which do not have the problem of spatial symmetry breaking by an unrestricted mean-field calculation. Reference data were taken from [50]. Figure 4 shows the IP for a chosen set of molecules. At first glance, the results resemble those for atoms in Fig. 2. The I_Δ provides reasonable results for all methods while I_ε shows dramatic differences between the LDA and the SIC models. However, taking a closer look, we also see that results for ADSIC and PZSIC show larger differences than in the case of atoms. Somewhat surprisingly, the ADSIC comes again much closer to experimental data than the PZSIC.
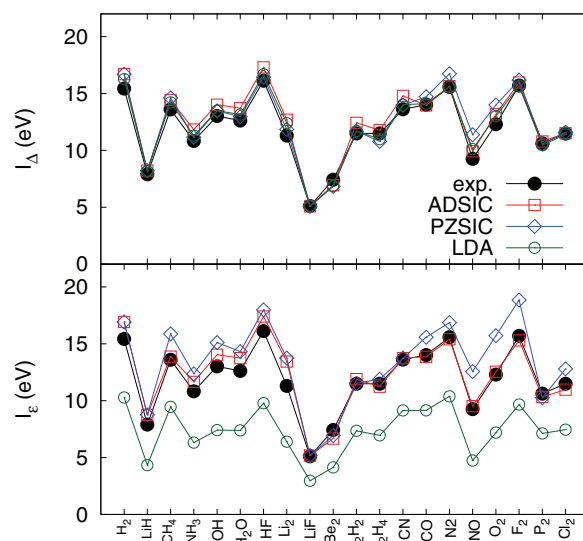

FIG. 4. (Color online) As in Fig. 2, but for a set of simple molecular systems.

Figure 5 shows the data from the previous figure in terms of energy differences, the errors ΔI as compared to reference data, and the NK energy. The results confirm the impressions indicated in the comparison of the IPs as such: The ΔI_ε shows significant differences between the PZSIC and ADSIC since the latter generally performs better.
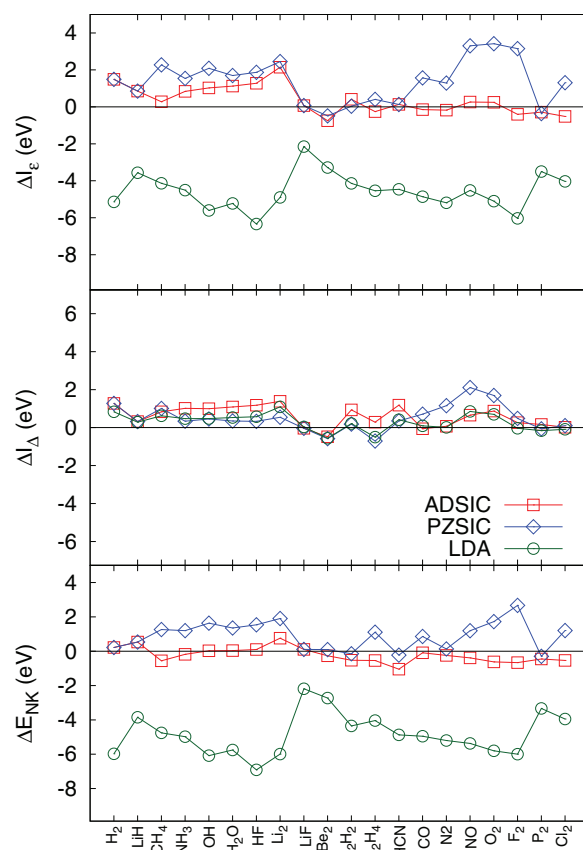

FIG. 5. (Color online) As in Fig. 3, but for a set of simple molecular systems.
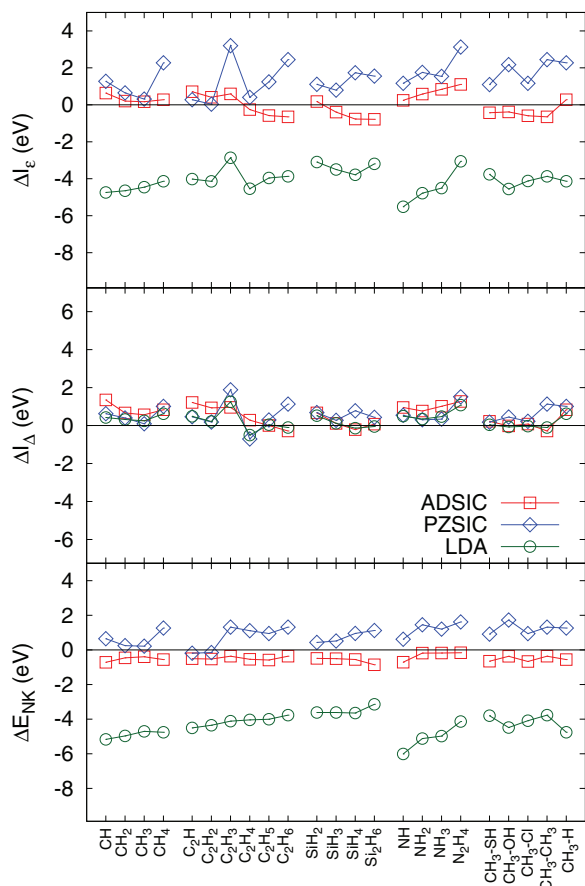
FIG. 6. (Color online) As in Fig. 3, but for families of molecules with systematically varied properties.

One may argue that comparison with reference data is also influenced by other details of the calculations or the choice of the reference data. The NK energy (bottom panel) is free of these uncertainties. The ADSIC clearly delivers the smallest NK energies. This was seen already for atoms. But here in the case of molecules the effect is even more pronounced as the PZSIC shows larger deviations.

D. Systematic sets of molecules

In this section, we look at a systematic variation of molecules, e.g., basic carbohydrates. The first family (CH$_x$) represents a variation of the number of C–H bonds. The second family changes the character (single, double, triple bonds) in C$_2$H$_n$. The third family is similar to the first one but carbon is replaced by a heavier element (silicon) with the same number of valence electrons, while the fourth series replaces the carbon atom by nitrogen (which has a different valence). In the final series one of the single-bonded hydrogen atoms in CH$_4$ is substituted by a different group. The last elements of the third and fourth series are not strictly within the systematics.

We saw in the previous systems that energy differences show more details than the energies as such. We thus proceed here immediately to energy differences, which are compiled in Fig. 6. The results are very similar to those in the previous case of simple molecules; see Fig. 5. Some of the deviations are, however, larger than in the previous case. This indicates that

these complex molecules are more critical test cases. Even in this more demanding scenario, we find again that the ADSIC performs better with respect to the deviation from reference data and even more so for the NK energies.

Thus we find that the ADSIC, which assumes orbital densities that are delocalized over the whole molecule, yields a systematic improvement over the PZSIC. This is somewhat surprising in view of the deficits of the ADSIC; in particular its inability to describe dissociation and the lack of size consistency are directly attributed to a too high level of delocalization.

For infinite matter, the ADSIC is not applicable due to the explicit dependence on the particle number. Already for larger systems, the explicit dependence on the total particle number quickly renders the SIC contribution to the energy functional an inefficient approach to cure problems of the LDA. The observation that delocalization on the length scale of small molecules is in fact favorable for the quality of the NK energy and IP calls for more systematic investigations.

E. Carbon rings and chains

The self-interaction error on the IP for the Coulomb Hartree term is typically of the order of e^2/R where R is the radius of the system. The error for the exchange-correlation potential can be estimated within the ADSIC as $v_{xc}[n/N]$. Both shrink with increasing system size. In order to explore the evolution of the self-interaction errors with increasing size, we consider carbon rings and chains. For the latter, we consider only odd numbers of atoms because only these molecules have stable electronic configurations for spin-saturated ground states. All the studied carbon rings are spin saturated in the neutral configuration. The geometries of the planar rings have been optimized on the GGA level (PW91) by allowing for relaxation of the atoms in the plane. The C–C bonds turn out to have more or less constant bond length. This means that increasing the number of carbon atoms induces a (linear) growth of the geometrical extension, of either the chain or the ring.

The upper two panels of Fig. 7 show the IPs for carbon rings as a function of the number of atoms. Comparing ADSIC and LDA results, we see again the equally good performance for I_Δ, and the large self-interaction error in I_ε for the LDA while the ADSIC behaves very well. The reference data, here the calculated LDA values I_Δ, show a pronounced step structure due to the successive filling of the electronic shells. Large I indicates particularly stable electronic structures, i.e., shell closures. Sudden reductions show that a new, and less bound, electronic shell has to be opened to place the given number of electrons. The LDA and ADSIC reproduce the shell effect. On first glance, the PZSIC results are quite surprising since they deviate even qualitatively from the other results, as they show less pronounced shell effects, at least with increasing chain length.

It should be noted that missing points also indicate that reliable minimization of the PZSIC energy becomes challenging for cationic configurations, where various local minima exist. The local minima correspond to different, almost energetically equivalent, configurations with different levels of delocalization of the unpaired electron in the spin-majority channel. The effect is worse for midshell systems but less
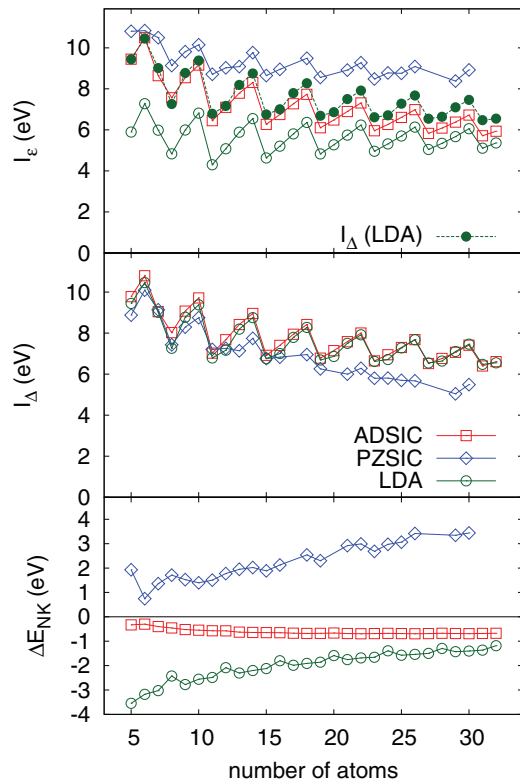
FIG. 7. (Color online) Non-Koopmans' energies (bottom) and ionization potentials I_Δ (from energy differences, middle) and I_ε (from the HOMO, top), computed in various schemes for carbon rings of various size ($5 \leqslant N_{\text{atoms}} \leqslant 32$). In the top panel, I_Δ from the LDA (see middle panel) is superimposed on the I_ε calculated in the LDA, ADSIC, and PZSIC.

FIG. 8. (Color online) As in Fig. 7 but for linear carbon chains ($3 \leqslant N_{\text{atoms}} \leqslant 11$). The data are complemented by results obtained from bare exchange-only Hartree-Fock calculations (triangles).

problematic for closed-shell configurations. No such problem exists for the ADSIC due to the absence of orbital dependence.

The lowest panel of Fig. 7 shows the NK energies. The ΔE_{NK} from the LDA starts large but shrinks with increasing size, as one could have expected. The ADSIC result is small throughout, but has a slight tendency to increase with size, and of course, never becomes larger than the error from LDA. However, the ΔE_{NK} from the PZSIC is generally large and even grows with system size. This finding is rather troublesome, as it confirms that the difference between the behavior of the LDA and ADSIC on the one hand, and the PZSIC on the other, actually stems from misconceptions in the PZSIC partially compensated in the approximate ADSIC.

The significant and positive NK energy indicates that strong correlation effects, which are underestimated in semilocal exchange and correlation, are overestimated by the PZSIC. The screening of such strong correlation effects has to be reintroduced in the self-interaction-corrected approach, e.g., by the assumption of more delocalized states, as in the case of the ADSIC.

The convergence of ADSIC and LDA results illustrates the collapse of the ADSIC as a working SIC scheme for extended systems, where $N \gg 1$, contrary to the case of small N where the NK energy is still improved significantly. The almost constant but finite NK energy indicates that, although the ADSIC is not capable of complete curing the
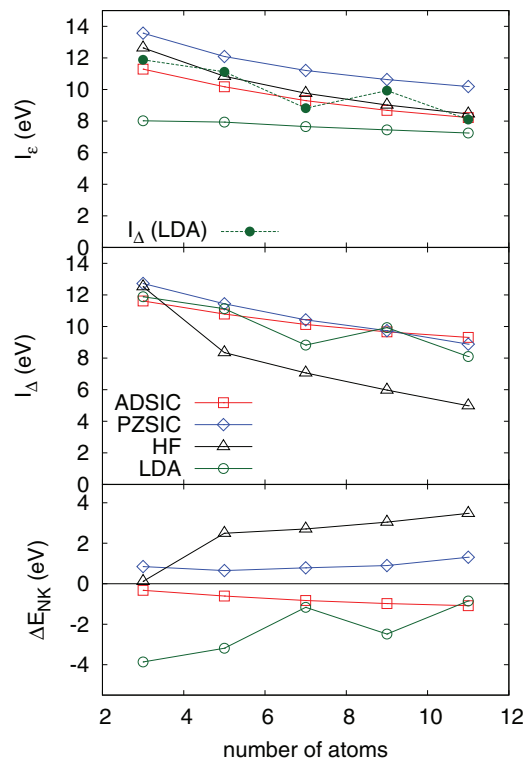
nonlinear dependence of the LDA energy functional for fractional occupation, it at least provides a scheme that yields similar magnitudes of errors for compact systems and extended ones, whenever the LDA is by itself considered a reasonable approximation there.

Figure 8 shows the IP and ΔE_{NK} for carbon chains. In this case, we added also results from a pure Hartree-Fock calculation. The PZSIC looks better here than for rings. But note that we have considered rather short chains. There are again large differences between PZSIC and ADSIC results. This time, however, they are distributed almost symmetrically around zero error (see the lowest panel). No clear preference can be deduced in this example.

The largest errors appear here for exact exchange in the HF calculation. Starting out perfectly for the smallest chain C_3, the NK energy already jumps for C_5 and continues to grow further. For the HF method, the effect can be understood due to the incomplete cancellation of the counteracting errors of the missing relaxation energy in the ion (due to the frozen-orbital approximation) and differences in the correlation energies of the charged and neutral species. With increasing system size, the relaxation energy of the open-shell cation increases, resulting in the significant errors observed. However, one has to note that such an argument would not apply in the Kohn-Sham framework, where Koopmans' condition should be necessarily fulfilled, i.e., all orbital relaxation and correlation effects are included in the position of the HOMO level. A detailed investigation would require calculations in the framework of the optimized effective potential method [37,38], for both

PZSIC and HF methods, which is beyond the scope of this paper.

F. Discussion

To summarize the results presented in the above figures, we have computed average errors for each group of system considered, atoms, simple molecules, and families of systematically varied molecules. Thereby, we distinguish between mean error ($\mathcal{E}_{\mathrm{mean}}$), mean absolute error ($\mathcal{E}_{\mathrm{MA}}$), and the error fluctuations (σ) defined as

$$\mathcal{E}_{\mathrm{mean}}(\Delta\mathcal{O}) = \frac{1}{N_{\mathrm{samp}}} \sum_i \Delta\mathcal{O}_i, \tag{10a}$$

$$\mathcal{E}_{\mathrm{MA}}(\Delta\mathcal{O}) = \frac{1}{N_{\mathrm{samp}}} \sum_i |\Delta\mathcal{O}_i|, \tag{10b}$$

$$\sigma(\Delta\mathcal{O}) = \frac{1}{N_{\mathrm{samp}}} \sum_i |\Delta\mathcal{O}_i - \mathcal{E}_{\mathrm{mean}}(\Delta\mathcal{O})|, \tag{10c}$$

where $\mathcal{O}$ is one of the considered observables, that is, I_Δ, I_ε, or E_{NK}. The index i runs over the N_{samp} samples in a given group, and $\Delta\mathcal{O}_i = \mathcal{O}_i - \mathcal{O}_i^{(\mathrm{ref})}$ stands for the observed deviation from the reference data $\mathcal{O}_i^{(\mathrm{ref})}$. The resulting averages for each group are listed in Table I. Computation of the IP as I_Δ, i.e., from energy differences, is always a safe procedure yielding reliable results already with the LDA. Computation as I_ε via the HOMO is possible with good accuracy in both SIC models. The great surprise is that the very simplistic ADSIC approach performs very well for the I_ε, typically even better than the PZSIC. The same conclusion is deduced from the non-Koopmans' energy ΔE_{NK}. This was already seen from the above figures and is corroborated in Table I on a quantitative level.

The excellent performance of the ADSIC in compact systems in terms of both accuracy and the small violation of Koopmans' condition is remarkable. Still, one should keep in mind the known deficiencies of the approach. Most notable is the violation of size consistency which becomes apparent

TABLE I. Mean error $\mathcal{E}_{\mathrm{mean}}$, mean absolute error $\mathcal{E}_{\mathrm{MA}}$, and error fluctuations σ as defined in Eqs. (IV F) for IPs as well as NK energy for the data sets shown in Figs. 3, 5, and 6. Redundant data in Fig. 6 are considered only once in the averages.

	I_Δ			I_ϵ			E_{NK}		
	$\mathcal{E}_{\mathrm{mean}}$	$\mathcal{E}_{\mathrm{MA}}$	σ	$\mathcal{E}_{\mathrm{mean}}$	$\mathcal{E}_{\mathrm{MA}}$	σ	$\mathcal{E}_{\mathrm{mean}}$	$\mathcal{E}_{\mathrm{MA}}$	σ
				Atoms					
LDA	0.2	0.3	0.3	−5.0	5.0	1.5	−5.1	5.1	1.6
PZSIC	0.3	0.3	0.3	0.7	0.8	0.7	0.4	0.5	0.5
ADSIC	0.4	0.5	0.4	0.2	0.4	0.4	−0.3	0.4	0.3
				Small molecules					
LDA	0.3	0.4	0.4	−4.6	4.6	0.7	−4.9	4.9	1.0
PZSIC	0.5	0.6	0.5	1.4	1.5	0.9	0.9	1.0	0.7
ADSIC	0.6	0.7	0.5	0.4	0.6	0.6	−0.2	0.4	0.3
				Systematic molecules					
LDA	0.3	0.4	0.3	−4.1	4.1	0.5	−4.3	4.3	0.5
PZSIC	0.5	0.6	0.4	1.4	1.4	0.7	0.9	0.9	0.4
ADSIC	0.5	0.6	0.4	0.1	0.5	0.5	−0.5	0.5	0.1

in the dissociation of a molecule. Consider a dimer with total electron number N which dissociates into one part containing N_1 electrons and another one with N_2 electrons. The ADSIC for the compound involves, of course, the total electron number N. Since we follow the dissociation path continuously, we necessarily have to keep using N in the correction. Finally, we end up with two isolated atoms which would be treated by one common correction still regulated by the total N. This is, of course, wrong as we know that each single atom has to be separately corrected with its own N_i. The case is even worse in violent dynamics leading to multifragmentation. The problem could already have been spotted from the fact that the dependence on $N = \int d^3\mathbf{r}\, n(\mathbf{r})$ implies a nonlocality which becomes increasingly problematic if $n(\mathbf{r})$ ceases to be compact, but is rather distributed over several regions of space.

Fully accomplished dissociation and multifragmentation are, of course, extreme limits. The defects of the ADSIC in this respect tend to show up earlier, for example, in the Born-Oppenheimer energies along the dissociation path. Thus one should not use the ADSIC for computing large-amplitude molecular vibrations without carefully checking its range of validity for the given application. Problems may also show up in molecules which combine very different length scales as, e.g., in NaH_2O where the Na atom adds a rather dilute electron distribution to the otherwise compact H_2O. In spite of the encouraging results presented above, one should check the NK energy ΔE_{NK} for each new application again.

These known shortcomings should not hinder us from appreciating the good performance attained by the ADSIC in structural and low-energy dynamical situations. As illustrated throughout the present work, the ADSIC provides a remarkable robustness in terms of Koopmans' violation. This implies, in particular, that it can be safely used in dynamical regimes where only a tiny fraction of an electron is emitted.

V. SUMMARY AND CONCLUSIONS

We have compared the performance of two different approaches to self-interaction correction regarding calculated ionization potentials and violation of Koopmans' theorem. We have focused the discussions on two SIC procedures: the original Perdew-Zunger approach (PZSIC) and the average density version thereof (ADSIC). A wide range of electronic systems has been considered ranging from atoms and simple molecules up to systematics of moderate-sized molecules, in particular carbon systems. The overall survey is thus quite general, so that the conclusions attained have a safe grounding, beyond any specific effect.

We find in all examples considered here that the ADSIC provides more reliable estimates of the IP and a smaller violation of Koopmans' theorem. This is a welcome result in view of the remarkable simplicity (and correlated low computational price) of ADSIC.

We have also explored a known collapse of the ADSIC approach for extended systems. It was shown that the PZSIC method also fails to cure flaws of the LDA in this regime. An optimistic interpretation of the data obtained on the example of carbon chains allows the conclusion that an efficient orbital-density-dependent SIC should provide weak localization of the single-electron states over several atoms. Such a weak

localization is in line with the excellent performance of the bare ADSIC in the case of the smaller molecules studied here.

Whereas the results of this survey question the quality of the PZSIC as a benchmark approach to a SIC, they simultaneously encourage the educated use of the much simpler ADSIC approach. However, as also noted, the ADSIC certainly does not provide the ultimate SIC scheme as it fails by construction, for example in the modeling of dissociation processes or strong ionization. The limits of the ADSIC with respect to dissociation or molecular structural rearrangement need to be explored further. Still it remains a viable and robust option for many dynamical situations, especially in the case of perturbative ionization, where the ionization potential, precisely the negative HOMO level, plays a central role. This implies that the ADSIC remains a favorable self-interaction correction in the calculation of reliable photoelectron spectra and angular distributions of emitted electrons, which represent an ever-growing issue in the dynamics of irradiated clusters and molecules.

Future work should also aim at investigating to what extent the level of localization can be controlled within the PZSIC scheme by modifying the functional form, e.g., within the framework of the GGA with SIC or by implying alternative localization criteria during the optimization of internal degrees of freedom, i.e., a unitary transformation among the single-particle states.

ACKNOWLEDGMENTS

[1] R. G. Parr and W. Yang, *Density-Functional Theory of Atoms and Molecules* (Oxford University Press, Oxford, 1989).

[2] R. M. Dreizler and E. K. U. Gross, *Density Functional Theory: An Approach to the Quantum Many-Body Problem* (Springer-Verlag, Berlin, 1990).

[3] W. Kohn, Rev. Mod. Phys. **71**, 1253 (1999).

[4] R. G. Parr and W. Yang, *Density-Functional Theory of Atoms and Molecules*, International Series of Monographs on Chemistry (Oxford University Press, New York, 1994).

[5] P.-G. Reinhard and E. Suraud, *Introduction to Cluster Dynamics* (Wiley, New York, 2004).

[6] *Time-Dependent Density Functional Theory*, edited by M. A. L. Marques, C. A. Ullrich, and F. Nogueira, Lecture Notes in Physics Vol. 706 (Springer, Berlin, 2006), p. 391.

[7] T. Fennel, K.-H. Meiwes-Broer, J. Tiggesbäumker, P. M. Dinh, P.-G. Reinhard, and E. Suraud, Rev. Mod. Phys. **82**, 1793 (2010).

[8] J. P. Perdew and A. Zunger, Phys. Rev. B **23**, 5048 (1981).

[9] H. B. Shore, J. H. Rose, and E. Zaremba, Phys. Rev. B **15**, 2858 (1977).

[10] K. Schwarz, Chem. Phys. Lett. **57**, 605 (1978).

[11] S. J. A. van Gisbergen, P. R. T. Schipper, O. V. Gritsenko, E. J. Baerends, J. G. Snijders, B. Champagne, and B. Kirtman, Phys. Rev. Lett. **83**, 694 (1999).

[12] S. Kümmel, L. Kronik, and J. P. Perdew, Phys. Rev. Lett. **93**, 213002 (2004).

[13] M. S. Hybertsen and S. G. Louie, Phys. Rev. B **34**, 5390 (1986).

[14] R. M. Nieminen, Curr. Opin. Solid State Mater. Sci. **4**, 493 (1999).

[15] M. Bär, L. V. Moskaleva, M. Winkler, P.-G. Reinhard, N. Rösch, and E. Suraud, Eur. Phys. J. D **45**, 507 (2007).

[16] P. M. Dinh, P.-G. Reinhard, and E. Suraud, Phys. Rep. **485**, 43 (2010).

[17] A. Pohl, P.-G. Reinhard, and E. Suraud, Phys. Rev. Lett. **84**, 5090 (2000).

[18] A. Pohl, P.-G. Reinhard, and E. Suraud, Phys. Rev. A **70**, 023202 (2004).

[19] U. De Giovannini, D. Varsano, M. A. L. Marques, H. Appel, E. K. U. Gross, and A. Rubio, Phys. Rev. A **85**, 062515 (2012).

[20] J. P. Perdew, R. G. Parr, M. Levy, and J. L. Balduz, Phys. Rev. Lett. **49**, 1691 (1982).

[21] J. P. Perdew and M. Levy, Phys. Rev. Lett. **51**, 1884 (1983).

[22] L. J. Sham and M. Schlüter, Phys. Rev. Lett. **51**, 1888 (1983).

[23] A. D. Becke, Phys. Rev. A **38**, 3098 (1988).

[24] J. P. Perdew, in *Electronic Structure of Solids 91*, edited by P. Ziesche and H. Eschrig (Akademie-Verlag, Berlin, 1991), p. 11.

[25] J. P. Perdew, K. Burke, and M. Ernzerhof, Phys. Rev. Lett. **77**, 3865 (1996).

[26] M. E. Casida and D. R. Salahub, J. Chem. Phys. **113**, 8918 (2000).

[27] J. P. Perdew, Chem. Phys. Lett. **64**, 127 (1979).

[28] M. R. Pederson, R. A. Heaton, and C. C. Lin, J. Chem. Phys. **80**, 1972 (1984).

[29] S. Goedecker and C. J. Umrigar, Phys. Rev. A **55**, 1765 (1997).

[30] V. Polo, E. Kraka, and D. Cremer, Mol. Phys. **100**, 1771 (2002).

[31] O. A. Vydrov and G. E. Scuseria, J. Chem. Phys. **121**, 8187 (2004).

[32] D. Hofmann, S. Klüpfel, P. Klüpfel, and S. Kümmel, Phys. Rev. A **85**, 062514 (2012).

[33] S. Klüpfel, P. Klüpfel, and H. Jónsson, Phys. Rev. A **84**, 050501 (2011).

[34] S. Klüpfel, P. Klüpfel, and H. Jónsson, J. Chem. Phys. **137**, 124102 (2012).

[35] A. Svane, Phys. Rev. B **53**, 4275 (1996).

[36] J. Messud, P. M. Dinh, P.-G. Reinhard, and E. Suraud, Phys. Rev. Lett. **101**, 096404 (2008).

[37] R. T. Sharp and G. K. Horton, Phys. Rev. **90**, 317 (1953).

[38] S. Kümmel and L. Kronik, Rev. Mod. Phys. **80**, 3 (2008).

[39] J. B. Krieger, Y. Li, and G. J. Iafrate, Phys. Rev. A **45**, 101 (1992).

[40] E. Fermi and E. Amaldi, Accad. Ital. Rome **6**, 117 (1934).

[41] C. Legrand, E. Suraud, and P.-G. Reinhard, J. Phys. B **35**, 1115 (2002).

[42] I. Ciofini, H. Chermette, and C. Adamo, Chem. Phys. Lett. **380**, 12 (2003).

[43] I. Ciofini, C. Adamo, and H. Chermette, Chem. Phys. **309**, 67 (2005).

[44] T. Koopmans, Physica (Utrecht) **1**, 104 (1933).

[45] P. Hohenberg and W. Kohn, Phys. Rev. **136**, B864 (1964).

[46] W. Kohn and L. J. Sham, Phys. Rev. **140**, A1133 (1965).

[47] L. A. Curtiss, K. Raghavachari, P. C. Redfern, and J. A. Pople, J. Chem. Phys. **106**, 1063 (1997).

[48] L. A. Curtiss, K. Raghavachari, G. W. Trucks, and J. A. Pople, J. Chem. Phys. **94**, 7221 (1991).

[49] C. Hartwigsen, S. Goedecker, and J. Hutter, Phys. Rev. B **58**, 3641 (1998).

[50] Russell D. Johnson III, "*NIST Computational Chemistry Comparison and Benchmark Database NIST Standard Reference Database Number 101 Release 14*", http://cccbdb.nist.gov/.

[51] J. Messud, P. M. Dinh, P.-G. Reinhard, and E. Suraud, Ann. Phys. (N.Y.) **324**, 955 (2009).

[52] P. E. Blöchl, Phys. Rev. B **50**, 17953 (1994).

[53] J. J. Mortensen, L. B. Hansen, and K. W. Jacobsen, Phys. Rev. B **71**, 035109 (2005).

[54] O. V. Gritsenko and E. J. Baerends, J. Chem. Phys. **120**, 8364 (2004).

[55] C.-H. Park, A. Ferretti, I. Dabo, N. Poilvert, and N. Marzari, arXiv:1108.5726.

[56] A. Valdes, J. Brillet, M. Graetzel, H. Gudmundsdottir, H. A. Hansen, H. Jonsson, P. Klüpfel, G.-J. Kroes, F. Le Formal, I. C. Man, R. S. Martins, J. K. Norskov, J. Rossmeisl, K. Sivula, A. Vojvodic, and M. Zach, Phys. Chem. Chem. Phys. **14**, 49 (2012).

[57] J. P. Perdew, J. A. Chevary, S. H. Vosko, K. A. Jackson, M. R. Pederson, D. J. Singh, and C. Fiolhais, Phys. Rev. B **46**, 6671 (1992).